Lawrence Berkeley National Laboratory

Lawrence Berkeley National Laboratory

Title

Effects of damping wigglers on beam dynamics in the NLC damping rings

Permalink

https://escholarship.org/uc/item/7tn3v36f

Authors

Wolski, Andrzej
Wu, Ying

Publication Date

2001-06-16

EFFECTS OF DAMPING WIGGLERS ON BEAM DYNAMICS IN THE NLC DAMPING RINGS*

A. Wolski[†], Y. Wu, LBNL, Berkeley, CA 94720, USA

Abstract

To achieve the required damping time in the main damping rings for the Next Linear Collider (NLC), a wiggler will be required in each ring with integrated squared field strength up to 110 T^2m [1]. There are concerns that nonlinear components of the wiggler field will damage the dynamic aperture of the ring, leading to poor injection efficiency. Severe effects from an insertion device have been observed and corrected in SPEAR 2 [2]. In this paper, we describe a model that we have developed to study the effects of the damping wiggler, compare the predictions of the model with actual experience in the case of the SPEAR 2 wiggler, and consider the predicted effects of current damping wiggler design on the NLC main damping rings.

1 WIGGLER REQUIREMENTS

The main damping rings (MDRs) for the NLC are designed to reduce the normalized beam emittances from 150 mm-mrad (horizontally and vertically), to 3 mm-mrad horizontally, and 0.02 mm-mrad vertically. With a repetition rate of 120 Hz, and three trains stored per ring, the damping must be achieved within 25 ms. The required vertical damping time is then 5 ms, and to achieve this requires the use of a strong wiggler. Some parameters relating to the wiggler design for the MDRs, are given in Table 1. More details on the damping ring complex and subsystems are given in references [1], [2]; the lattice design for the main damping rings is described in [3].

Table 1: MDR Damping Wiggler Parameters

Beam energy	1.98 GeV
Wiggler peak field	2.15 T
Wiggler period	0.27 m
Total wiggler length	46.25 m
Energy loss/turn from dipoles	247 keV
Energy loss/pass from wiggler	530 keV
Damping times $\tau_{x,y,\varepsilon}$	4.85, 5.09, 2.61 ms

Another principal requirement of the damping rings is that they have sufficient dynamic aperture to allow good injection efficiency. Nonlinear components in the wiggler field can limit the dynamic aperture, as was recently seen at SPEAR 2 [4]. For analysis of the dynamics, it is desirable to have a physical model of the wiggler field that reproduces the nonlinear components with good accuracy, and allows fast symplectic tracking. Codes

already exist that numerically integrate the equations of motion through the wiggler, but this can take several hours, and produces limited analytical information. We have pursued an alternative approach, based on the construction of a symplectic integrator for the field expanded in a series of modes. This allows an analysis of the dynamic effects of the wiggler to be produced in minutes rather than hours, and provides potentially useful information connecting the field quality with the dynamics, in terms of the mode coefficients.

The characterization of the wiggler then consists of two steps:
- determine the mode coefficients from (modeled or measured) field data;
- track through the wiggler, using the mode coefficients in an appropriate symplectic map.

2 FITTING THE WIGGLER FIELD

We consider the case where the magnetic vector potential in the wiggler field can be expressed as:

$$A_x = \sum_{m,n} c_{mn} \frac{1}{nk_z} \cos(mk_x x) \sin(nk_z z) \cosh(k_{y,mn} y)$$
$$A_y = \sum_{m,n} c_{mn} \frac{mk_x}{nk_z k_{y,mn}} \sin(mk_x x) \sin(nk_z z) \sinh(k_{y,mn} y) \tag{1}$$
$$A_z = 0$$

where $k_z = 2\pi/\lambda_w$, and λ_w is the wiggler period. Maxwell's equations are satisfied if we impose the conditions:

$$k_{y,mn}^2 = m^2 k_x^2 + n^2 k_z^2$$

The potential (1) is not the most general form; we have imposed symmetry conditions (i.e. neglected random construction errors) to eliminate several sets of modes, for example. Also, we have made the field periodic in x, which we can do by setting $k_x = \pi/2L_x$, where the field is known between limits $\pm L_x$. The field components are readily derived from the potential (1). In particular, we see that a wiggler with a purely sinusoidal field variation along the z axis has a single n mode, and $\Sigma c_{m1} = B_w$, where B_w is the peak field.

Imposing the periodicity in x is useful, since it allows us to determine the coefficients c_{mn} from field data in the x-z plane simply by using a 2-dimensional Fourier transform. Representing the field using a finite number of modes will give some error, which will be small for $y=0$, but will increase exponentially with y as a result of the hyperbolic function in (1). The error comes largely from the higher order modes in the expansion; fortunately, these modes make only a small contribution to the fit in the x-z plane,

so by making small changes to the coefficients with large m and n, we can greatly improve the fit in y without degrading the fit in x or z significantly.

To determine the corrections to the coefficients, we begin by constructing a vector $\vec{c}$, whose components c_j are just the coefficients c_{mn} listed in any order. We then write the vertical component of the field at a point y_i as:

$$B_y(y_i) = \sum_j \cosh(k_{y,j} y_i) c_j$$

Constructing a vector $\vec{B}_y$ by selecting a set of points $\{y_i\}$, and considering changes Δc_j in the mode coefficients, we then define an "error vector":

$$\Delta \vec{B}_y = \mathbf{F} \cdot \Delta \vec{c}$$

where $\mathbf{F}$ is a matrix with components $F_{ij} = \cosh(k_{y,j} y_i)$. In general $\mathbf{F}$ is not square, or may be close to singular; the required corrections to the mode coefficients must then be determined from the error vector by singular value decomposition.

Using this technique, we find that we can fit the field data for the SPEAR BL11 wiggler to within a few tens of gauss using 32 modes, and can fit the field data for the damping ring hybrid wiggler to within a few gauss using 79 modes. Although we fitted directly only the vertical field component, the horizontal and longitudinal components are also well described by the resulting expansion.

3 SYMPLECTIC INTEGRATORS

We proceed to derive a map describing the particle dynamics in the wiggler. We begin with the standard Hamiltonian:

$$H = -\sqrt{(1+\delta)^2 - (p_x - a_x)^2 - (p_y - a_y)^2} - a_z$$

We choose a gauge $a_z = 0$ and expand for $(p_i - a_i)^2 \ll 1$:

$$H \approx -(1+\delta) + \frac{p_x^2 + p_y^2}{2(1+\delta)} + \frac{a_x^2 + a_y^2}{2(1+\delta)} - \frac{a_x p_x + a_y p_y}{(1+\delta)} \quad (2)$$

The first two terms in (2) generate a drift, and the third term generates a transverse momentum "kick". The fourth term makes a small contribution if we average the Hamiltonian over one period of the wiggler. We note that it is possible to construct an explicit integrator for general Hamiltonians of the form (2) [5]. We consider the simplified case, where the map through one period, is generated by:

$$H_{\text{kick}} = \frac{\langle a_x^2 \rangle + \langle a_y^2 \rangle}{2(1+\delta)} \quad (3)$$

with $a = A/B\rho$, and the potential A is given by (1). In the special case of infinitely wide pole pieces, we find that there is a linear focusing:

$$K_1 = \frac{1}{2(1+\delta)(B\rho)^2} \sum_n c_n^2 = \frac{1}{\lambda_w (1+\delta)(B\rho)^2} \int_0^{\lambda_w} B^2 \, ds$$

which agrees with the hard-edged dipole model of the wiggler.

One problem with using the full form for the symplectic integrator given in (3) is that a large number of terms need to be evaluated, so tracking can be very slow. By using some approximations, we can develop a somewhat more efficient model. Let us neglect for the moment all field modes apart from the fundamental, and assume that the trajectory of a particle through the period is close to sinusoidal. The integrated field seen by a particle entering at $x = x_0$, $y = 0$, is then given by (we consider $\delta = 0$):

$$\int B_y \, ds = B_w \int_0^{2\pi/k_z} \cos(k_z z) \cos(x_0 + a \cos(k_z z)) \, dz \quad (5)$$
$$= -B_w \lambda_w \sin(x_0) J_1(a)$$

where

$$a = \frac{B_w \cos(k_x x_0)}{(B\rho)^2 k_z^2}$$

The integrated field from (5) gives the horizontal momentum kick. To take account of the full set of field modes, we propose the following form for the Hamiltonian:

$$H_{\text{kick}} = \frac{1}{2B\rho} \sum_{mn} c_{mn} \cos(m k_x x) J_n(f) \cosh(k_{y,mn} y) \quad (6)$$

where

$$f = \frac{B_y(x, y, z = 0)}{(B\rho) k_z^2}$$

In the case of infinitely wide pole pieces, and a single longitudinal mode, we find

$$\underset{k_x \to 0}{Lt} H_{\text{kick}} = \frac{\hat{B}_w^2 \cosh^2(k_z y)}{4(B\rho)^2 k_z^2}$$

so we again have the correct linear focusing. The reduced model expressed in (6) involves summation over a significantly smaller number of terms than the full integrator (3).

To verify the validity of the approximations leading to the reduced model (6), we consider the case of SPEAR 2 BL11, which shows very strong nonlinear effects. As can be seen in Figure 1, the two symplectic integrator models are in excellent agreement with the numerical integration, for the horizontal kick and for $y = 0$. The lower diagram shows the vertical kick as a function of x, for $y = 0.003$ m. The agreement is less precise, but still sufficiently good to give us some confidence in our symplectic integrators. We find that the different models yield very similar results for the effect of BL11 on such quantities as the tune shift with amplitude, closed orbit shift with momentum, and dynamic aperture.
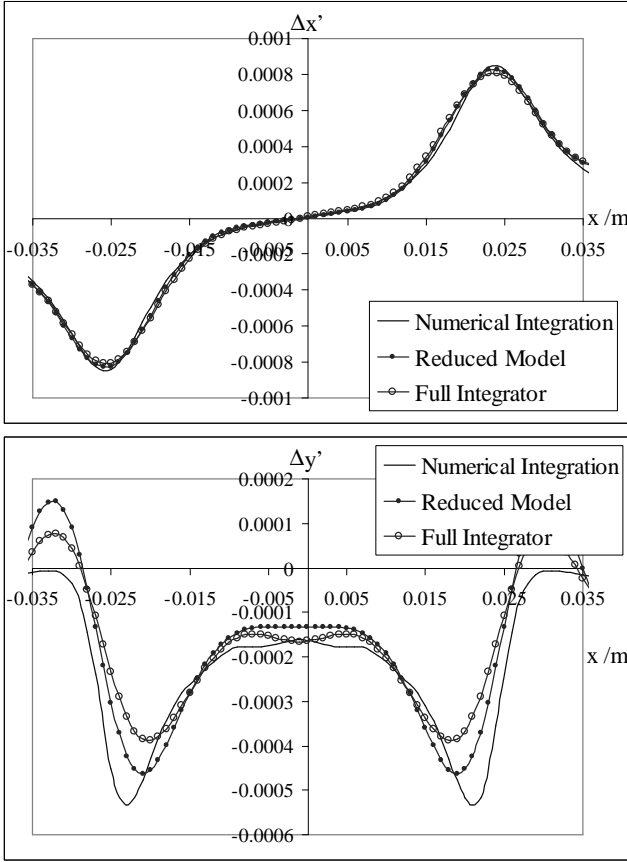
Figure 2: Horizontal momentum kick from one period of the NLC main damping rings wiggler.

Figure 1: Horizontal and vertical kicks from one period of the SPEAR 2 BL11 wiggler.

4 THE NLC DAMPING RING WIGGLER

In the case of the NLC main damping ring wiggler, we do not have results from numerical integration available. However, the nonlinear effects are much less severe than the case of the SPEAR BL11 wiggler, and as we have already shown, the two symplectic integrator models give the correct behavior for an ideal wiggler in the linear limit. The horizontal momentum kick derived from each model at $y=0$ is shown in Figure 2. Reasonable agreement is shown for the vertical momentum kick, and for $y\neq0$.

The half gap of the wiggler in the NLC MDRs is 9 mm; this is well within the dynamic aperture of the lattice, modeling the wiggler as a linear element. Thus, when tracking through the nonlinear wiggler field, we are forced to collimate the beam at the limits of the known field data.

The apertures in the cases for a linear and nonlinear wiggler (using the reduced symplectic integrator) are shown in Figure 3; the pole gap of the wiggler is also shown, scaled by the vertical beta function to the observation point. We include nonlinear effects from the sextupoles and vertical collimation at the wiggler, and obtain essentially the same aperture for both linear and nonlinear wiggler. We conclude that the nonlinear components of the wiggler field in the NLC damping rings do not have significant effects within the physical aperture of the wiggler.
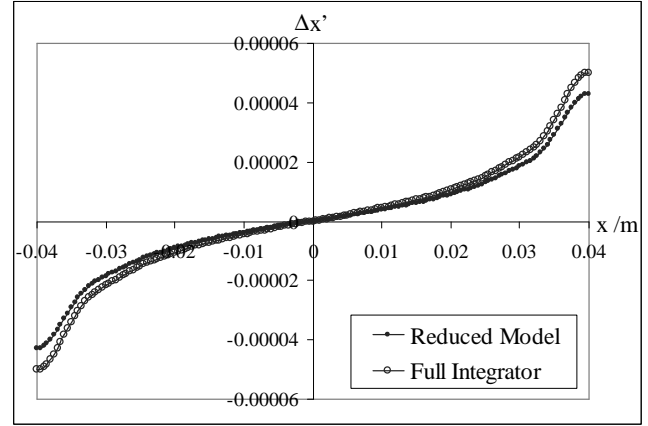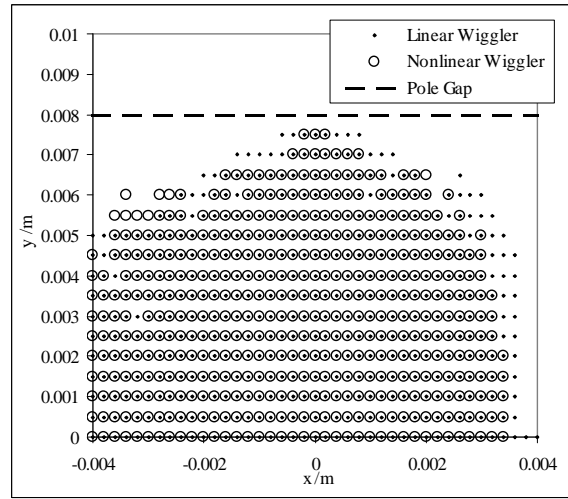

Figure 3: Aperture with the linear and nonlinear wiggler models, and vertical collimation in the wiggler.

The restricted physical aperture of the wiggler is a concern for the acceptance of the ring. More rigorous tracking studies are planned to determine the losses, and hence the radiation load, at the wiggler.

5 ACKNOWLEDGEMENTS

5 REFERENCES

[1] J.N. Corlett et al, "The Next Linear Collider Damping Ring Complex", these proceedings.
[2] J. Sheppard et al, "Update to the Next Linear Collider Injector System Design", these proceedings.
[3] A. Wolski and J.N. Corlett, "The Next Linear Collider Damping Ring Lattices", these proceedings.
[4] J. Safranek et al, "Nonlinear Dynamics in SPEAR Wigglers", proceedings EPAC 2000.
[5] Y. Wu et al, "Symplectic Models for General Insertion Devices", these proceedings.